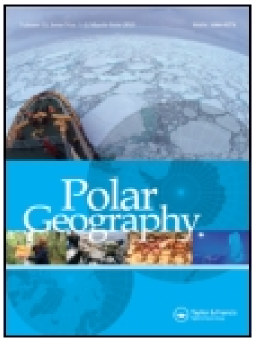

Taylor & Francis
Taylor & Francis Group

Polar Geography

ISSN: 1088-937X (Print) 1939-0513 (Online) Journal homepage: http://www.tandfonline.com/loi/tpog20

Spatial variability of permafrost active-layer thickness under contemporary and projected climate in Northern Alaska

Dmitry A. Streletskiy , Nikolay I. Shiklomanov & Frederick E. Nelson

Polar Geography
Vol. 35, No. 2, June 2012, 95–116

Spatial variability of permafrost active-layer thickness under contemporary and projected climate in Northern Alaska

DMITRY A. STRELETSKIY[a]*, NIKOLAY I. SHIKLOMANOV[a] and FREDERICK E. NELSON[b]

[a]*Department of Geography, George Washington University, 1922 F St NW Washington, DC 20052, USA;*
[b]*Department of Geography, University of Delaware, Newark, DE 19711, USA*

The active layer plays an important role in the functioning of environmental ecosystems and affects many human activities in the polar regions. Regional assessments and predictions of this parameter are critical for many physical and social applications. Large heterogeneity in near-surface permafrost characteristics, including the active layer, even over small distances, creates serious constraints to their evaluation across large geographic extents. Discrepancies between modeled climatic fields add to the uncertainties associated with predicting active-layer thickness (ALT) at regional scales. This study uses a stochastic approach, in combination with an equilibrium permafrost model, to map the geographic distribution of ALT and near-surface permafrost temperature on the North Slope of Alaska. GIS techniques are used to determine the spatial variability of ecosystem factors controlling the ground thermal regime within each grid cell of the permafrost model. To incorporate the uncertainty associated with the climate data, the model was forced by four sets of gridded air temperature fields used widely in spatial modeling applications. A series of calculations created a spectrum of possible solutions for ALT and associated probability ranges for each grid cell. Results are presented as a series of maps depicting geographic patterns of contemporary and future ALT for the North Slope of Alaska.

Introduction

Although uncertainties exist about future climate change, the warming observed over the land masses of the Arctic during recent decades is creating profound changes in cold regions (e.g. ACIA 2004; Hinzman *et al.* 2005). Major future impacts driven by global greenhouse warming are likely to include changes in the ground thermal regime and related consequences for ecosystems and humans. Climatic change in the Arctic results in increases of soil temperature (Romanovsky *et al.* 2010), accompanied by contraction of the extent of permafrost (Oberman and Shesler 2009). Some of these changes will have positive ramifications, but most are likely to be detrimental. Increased soil temperature may promote *thermokarst*, differential subsidence caused by melting of the excess ice common in upper permafrost layers in many high-latitude regions. Permafrost warming and development of thermokarst terrain can result in widespread hydrological and ecological disturbance (Callaghan *et al.* 2011; Gutman and Reissell 2010) and disruption of

*Corresponding author. Email: strelets@gwu.edu

Polar Geography
ISSN 1088-937X print/ISSN 1939-0513 online © 2012 Taylor & Francis
http://www.tandfonline.com
http://dx.doi.org/10.1080/1088937X.2012.680204

existing infrastructure (ACIA 2004; Nelson *et al.* 2002; Streletskiy *et al.* 2012). A progressive increase in the thickness of the seasonally thawed layer above permafrost (the *active layer*) could be a relatively fast reaction to climatic warming, and may facilitate further climate changes through release of the large amount of carbon stored in northern soils (Schuur *et al.* 2008).

Information about the geographic variation of active-layer thickness (ALT) can be obtained by extensive sampling, estimated indirectly from remotely sensed observations, or simulated by models. Despite rapid growth in its observation network, however, geocryology remains a data-limited science. Significant efforts have been made to derive the spatial distribution of permafrost parameters computationally (Anisimov and Reneva 2006; Anisimov *et al.* 1997; Arzhanov *et al.* 2007; Lawrence and Slaten 2005, 2008; Malevsky-Malevich *et al.* 2006; Marchenko *et al.* 2008; Nelson *et al.* 1997; Sazonova and Romanovsky 2003; Shiklomanov and Nelson 1999, 2002; Wisser *et al.* 2011). One of the major roles of spatial permafrost models is to generate areal datasets of the active layer, which can be used for a wide range of hydrologic, ecological, climatological, and socioeconomic assessments in the terrestrial Arctic. Although the methods used to produce such maps differ in complexity, data requirements, and applicability to different geographic scales, they can only produce estimates of thaw depth based on consideration of those processes explicitly considered in the model, regardless of the level of natural variability. This is an especially difficult problem for permafrost research focused on small geographical scales (i.e. over large areas), in which coarse geographic resolution and scarce observational data in the Arctic preclude realistic representation of the substantial variability known to occur at local scales (e.g. Nelson *et al.* 1999).

Permafrost modeling becomes even more complex when climatically driven changes in the heterogeneous permafrost parameters are addressed. Most current global climatic fields lack local detail, owing to their coarse resolution (e.g. $0.5 \times 0.5^{\circ}$ or 25×25 km). This results in a dramatic discrepancy between the level of spatial detail provided by currently available climate fields and that required by permafrost impact models. Despite these difficulties, some successful attempts have been made to predict future permafrost conditions based on global (Anisimov *et al.* 1997, 2002) and regional climatic scenarios in West Siberia (Duchkov and Balobaev 1998), East Siberia (Stendel *et al.* 2006), the Russian Arctic (Anisimov and Reneva 2006; Arzhanov *et al.* 2007; Pavlov 1994), and Alaska (Marchenko *et al.* 2008; Romanovsky and Osterkamp 2001; Sazonova and Romanovsky 2003; Shiklomanov and Nelson 2002).

However, the vast majority of spatial active-layer models provide estimates without supporting information about reliability or geographic variation. Alternatively, a description of model uncertainty may allow evaluation of the range and variation of potential model results. Assessment of model uncertainties is especially important for climate-change applications. Any regional changes in thaw depth attributable to global warming should fall outside the range of variations associated with uncertainties inherited from the spatial active-layer model. Evaluation of regional characteristics and trends will also significantly narrow the gap between small-scale climate models and active-layer observations conducted at local scales. This study is concerned with developing a practical methodology for quantitative description of the uncertainties associated with spatial active-layer estimates. The work utilizes available observational data, GIS, and modeling techniques to evaluate the spatial variability of ALT under observed and projected climate change in Northern Alaska (figure 1).

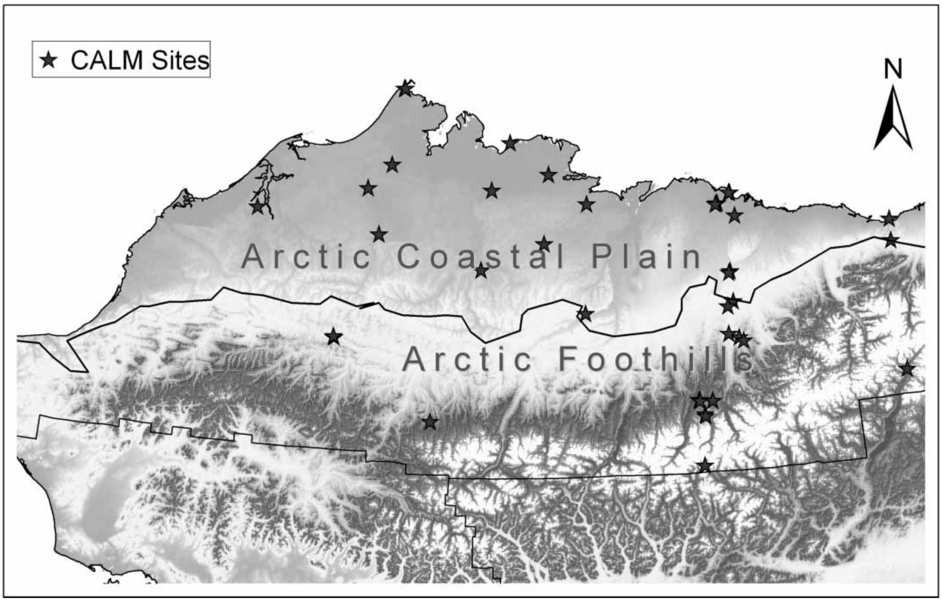

Figure 1. The North Slope of Alaska and geographic distribution of Alaskan CALM observational sites used in this study.

Methodology

Permafrost model

Calculations for this study were carried out using a permafrost model based on Kudryavtsev *et al.*'s (1974) formulation. This approach takes into account major geological and geographical factors and assumes a periodic, quasi-steady-state temperature regime. It describes the exponential attenuation of the temperature oscillations in the snow cover and vegetation, and takes into account the temperature offset in the uppermost soil layer of seasonal thawing. The maximum depth of thawing and ground temperature are calculated in the model by means of an analytically derived solution to the soil heat conduction problem assuming a homogeneous layer of permafrost in the thermodynamic equilibrium with the atmospheric climate. For this study, Kudryavtsev *et al.*'s algorithm was modified to take into account the presence of an organic layer (peat) underlain by mineral soil. The thermal characteristics of each layer in the frozen and thawed states are different and assigned by granulometric and soil moisture content parameterization. The model requires a minimal set of forcing data, including the annual mean and the amplitude of the air temperature, snow depth, volumetric heat capacities and thermal conductivities of snow, vegetation, and soil. Computational details are provided in Anisimov *et al.* (1997) and Shiklomanov and Nelson (1999).

Owing to their relative simplicity and low data requirements, models based on Kudryavtsev *et al.*'s formulations have been used frequently in conjunction with GIS technology to assess both ALT and mean annual ground temperatures at regional (e.g. Shiklomanov and Nelson 1999) and circumarctic (e.g. Anisimov *et al.* 1997) scales and to estimate the long-term response of permafrost to changes in climate (e.g. Sazonova and Romanovsky 2003). The results from comparison of several spatial active-layer models (Shiklomanov *et al.* 2007) indicate that Kudryavtsev-based equilibrium models provide an economical approach that can be used for accurate spatial and temporal characterization of major permafrost parameters at regional, continental, and hemispheric scales.

Climatic input

The distribution of Arctic stations used as sources of input data for active-layer modeling is uneven, and the duration of records varies substantially from station to station. These facts are responsible for the current inability to estimate regional active-layer fields directly from observational data. This problem is frequently addressed by transforming the observational data to regularly spaced grids (e.g. Willmott and Matsuura 1995). Gridded datasets are widely used to compute regional and global climatic variables and have become the dominant form of input to modeling procedures, including active-layer and permafrost modeling. The results are, to a large extent, dependent on the particular dataset used as climatic input.

To incorporate the uncertainty associated with the climate data, the model was forced by four commonly used sets of gridded air temperature fields at 625 km^2 resolution. The gridded datasets used in this study were developed at the University of Delaware (Willmott and Matsuura 2001; hereafter W&M); the University of East Anglia, UK Climate Research Unit (Mitchell and Jones 2005; hereafter CRU); the European Center for Medium-Range Weather Forecast 40-year Re-Analysis (Uppala *et al.* 2005; hereafter ERA40); and the National Center for Environmental Prediction–National Center for Atmospheric Research (Kalnay *et al.* 1996; NCEP–NCAP, hereafter NCEP).

Active-layer thickness varies according to fluctuations of climatic conditions, reflecting heat and moisture exchange between the atmosphere and the ground during particular years. Over a period of several years, the active layer statistically approaches its climatically determined mean thickness. If climatic change occurs, the active layer changes accordingly, establishing a new mean equilibrium thickness. To evaluate present geographic patterns of the active layer, the model was forced by monthly air temperature for the 1970–2000 period, using the four climatic datasets referenced above.

Snow cover

The effect of snow cover on the ground thermal regime depends on time, snow depth, and the physical properties of snow, such as density and texture (Zhang *et al.* 1997). Snow cover tends to attenuate the amplitude of the mean annual ground surface temperature, relative to the air temperature amplitude (e.g. Goodrich 1982; Sazonova and Romanovsky 2003). While several parameterizations of snow thermal conductivity can be used to evaluate thermal effect of snow cover in the model, the absence of regional data on initial snow density and its progression through winter significantly limits incorporation of realistic snow parameterization in Northern Alaska. Sensitivity analysis has shown, however, that ALT is quite conservative to changes in this parameter at the annual scale (Streletskiy 2010). Snow thermal conductivity was therefore assigned an average value of 0.21 W/m°C (Table 1). This

Table 1. Thermal properties of snow, low vegetation cover, peat and mineral soil.

Type	γ_p (kg/m^3)	W_p	$\lambda_{\tau p}$ (W/mC)	λ_{fp} (W/mC)	$C_{\tau p}$ (kJ/m^{3}C)	C_{fp} (kJ/m^{3}C)	K_{th} ($\times 10^{-6}$ m^2/s)	K_{fr} ($\times 10^{-6}$ m^2/s)	Source
Snow	300			0.21		2090		0.34	Sturm *et al.* (1997)
Turf (grass)		Dry	0.4	0.5					Chernad'ev (1984)
Turf (grass)		Moist	0.51						Shender (1986)
Forest litter			0.163						Shender (1986)
Forest litter (black spruce)			0.03–0.088						Sharrat (1997)
Moss		Dry	0.174	0.174					Chernad'ev (1984)
Moss			0.37						Beringer (2001)
Moss		Dry	0.1						Hinzman (1991)
Moss		Sat	0.6						Hinzman (1991)
Eriophorum vaginatum	890	Sat	0.55	1.69	3520	2200	0.16	0.77	Feldman (1977)
E. vaginatum	930	Dry	0.198	0.233					Chernad'ev (1984)
Sphagnum lindbergi	820	Sat	0.41	1.4	3200	2100	0.13	0.67	Feldman (1977)
Sphagnum		Dry	0.233	0.384					Chernad'ev (1984)
Sphagnum		Wet	0.384	0.768					Chernad'ev (1984)
Sphagnum		Sat	0.582	1.163					Chernad'ev (1984)
Sphagnum		Dry	0.04						Brown and Williams (1972)
Sphagnum		Sat	1.1						Brown and Williams (1972)
Sphagnum		Dry	0.152–0.219						Shender (1986)
Sphagnum		Sat	0.3–0.56						Shender (1986)
Peat			0.23–0.93	0.93–1.28					Ershov (2002)
Peat	920	11.7	0.44	1.62	3700	2352	0.12	0.69	Feldman *et al.* (1988)
Peat	900	4	0.41	1.63	3235	2100	0.13	0.78	Feldman *et al.* (1988)
Peat	930	4.4	0.4	1.57	3440	2185	0.12	0.72	Feldman *et al.* (1988)
Peat	920	8.5	0.37	1.4	3486	2184	0.11	0.64	Feldman *et al.* (1988)
Peat	950	13.4	0.53	1.77	3800	1980	0.14	0.89	Feldman *et al.* (1988)
Peat	300	0	0.06		576		0.10		Williams and Smith (1989)
Peat	700	0.57	0.29		2310		0.13		Williams and Smith (1989)
Peat	1100	0.72	0.5		4015		0.12		Williams and Smith (1989)

Table 1. (Continued).

Type	γ_p (kg/m^3)	W_p	$\lambda_{\tau p}$ (W/mC)	λ_{fp} (W/mC)	$C_{\tau p}$ (kJ/m^{3}C)	C_{fp} (kJ/m^{3}C)	K_{th} ($\times 10^{-6}$ m^2/s)	K_{fr} ($\times 10^{-6}$ m^2/s)	Source
Peat (Carex)		Wet	0.23–0.28	0.43–0.67					Kujala *et al*. (2008)
Peat (Carex)		Sat	0.41–0.5	1.48–1.49					Kujala *et al*. (2008)
Peat		Dry–wet	0.05–0.25	0.07–0.40					Konovalov and Roman (1973)
Peat		Wet–sat	0.25–0.81	0.40–1.1					Konovalov and Roman (1973)
Sand	1300								
Sandy loam	1350								
Loam	1380								
Silt	1400								
Clay	1500								

value was derived from 354 observations published from 1889 to 1997, summarized by Sturm *et al.* (1997).

Landcover

Both moss and vascular vegetation influence the thermal regime of the ground significantly. Vegetation acts as a thermal insulator between the atmosphere and the ground. It also affects the redistribution of snow cover. Depending on geographical conditions, a vegetation cover can have either a warming or a cooling influence on the ground (Kudryavtsev *et al.* 1974). In Northern Alaska, increased plant biomass along the bioclimatic gradient tends to have a cooling influence, owing to the increase in summer insulation (Walker *et al.* 2003). The effect of vegetation on the ground thermal regime was estimated using Ershov's (2002, pp. 332–339) approach. Ershov's approach involves calculating changes in annual temperature (ΔT_v) and amplitude (ΔA_v) attributable to the presence of vegetation during warm and cold period of the year. It does not directly account for phase changes in vegetation cover. Annual temperature variation is approximated by a sinusoidal function divided by two temperature harmonics around 0°C with periods of $2\tau_w$ (warm period) and $2\tau_c$ (cold period) and corresponding amplitudes of A_w and A_c.

Based on Fourier's law, the amplitude decay due to presence of vegetation cover can be found as:

$$\Delta A_v = \frac{\Delta A_c \tau_c + \Delta A_w \tau_w}{\tau}$$

$$\Delta T_v = \frac{\Delta A_w \tau_w - \Delta A_c \tau_c}{\tau} \frac{2}{\pi}$$

where ΔA_c and ΔA_w are differences in temperature amplitudes above and below vegetation cover for the cold and warm periods, respectively, τ_w and τ_c represent the duration of the warm and cold periods, (s), and τ is the length of the annual period (s). The first two quantities are calculated by:

$$\Delta A_w = A\left(1 - e^{-z\sqrt{(\pi/(2\tau_w K_t))}}\right), \quad A_w = A + T$$

$$\Delta A_c = A\left(1 - e^{-z\sqrt{(\pi/(2\tau_c K_f))}}\right), \quad A_c = A - T$$

where z is the height of the vegetation (m), K_t and K_f are thermal diffusivity of vegetation for the warm and cold periods, and A and T are thermal amplitude and temperature in the air, respectively. Based on the above formulations, the combined thermal effect of vegetation (ΔT_v) can be negative or positive depending on whether winter ($\Delta A_c \tau_c$) component is higher than summer one ($\Delta A_w \tau_w$). The simplified equation can also be used to evaluate the thermal influence of snow, in which case $\Delta A_w \tau_w$ is equal to zero.

Thermal properties of organic soil

Peatlands are widespread in the Northern Hemisphere, covering 4 million km^2 (MacDonald *et al.* 2006). The thickness of the peat layer is usually between 10 and 60 cm, but can be as much as 2 m in the polygonal peatlands of Siberia. Despite its thermal significance, peat is rarely considered explicitly in land-surface models (Beringer *et al.* 2001). Nelson (1986) demonstrated the importance of peatlands in the context of permafrost modeling at regional scales. Although the importance of peatlands for the formation and maintenance of permafrost has long been known (Brown 1970; Nelson 1986; Nelson *et al.* 1985; Riseborough and Burn 1988), only recently has the presence of peat begun to be understood as an important part of global climate and permafrost models (Lawrence and Slater 2008; Wisser *et al.* 2011).

We analyzed a range of published values on the thermal properties of forest litter, green and Sphagnum mosses, and peat collected from different parts of the Arctic (Table 1), including Finland (Kujala *et al.* 2008), West Siberia and Russian Far East (Feldman *et al.* 1988), Alaska (Sharrat 1997), as well as published results from laboratory experiments (e.g. Ershov 2002; Konovalov and Roman 1973). The thermal properties of peat depend on its density and gravimetric water content. The conductivity of thawed peat varies from 0.05 to 1.1 W/m°C depending on soil moisture, with an estimated average value of 0.38 W/m°C; the thermal conductivity of frozen peat is much higher (0.07–1.8 W/m°C), with an estimated average of 1.28 W/m°C. The thermal conductivity of frozen peat increases with gravimetric moisture content and density. Peat density of 300 kg/m^3 was assumed. Thermal conductivity and volumetric heat capacity in the model for frozen and thawed moss were set to values obtained by Feldman (1977) for *Eriphorium vaginatum* and *Sphagnum lindbergi*.

Thermal properties of mineral soil

Bulk density, soil moisture content, amount of unfrozen water, thermal conductivity, and heat capacity are required to estimate heat transfer in soils. There are numerous empirical and semi-empirical methods to estimate the thermal conductivity of soil (e.g. Farouki 1981; Gavriliev 2003). However, most of the methods require parameters, such as quartz content, amount of unfrozen water, and organic content, that cannot be assessed adequately at regional scales. This study utilizes empirical data from the *Russian Construction Norms and Regulations* (CNR 1990) and Feldman *et al.* (1988). Mineral densities of main classes of mineral soil are presented in Table 1. The thermal conductivity of the ground increases with soil moisture content and is prescribed independent for thawed and frozen states. If the thermal conductivities of frozen and thawed soil are unequal, a thermal offset occurs, as the total amount of heat needed for phase changes and actual heating of the ground is different at positive and negative temperatures. The thermal offset was calculated following Sazonova and Romanovsky (2003). Temperature at the bottom of the active-layer and ALT was calculated using Kudryavtsev *et al.*'s equations (1974), specified in Anisimov *et al.* (1997) and Romanovsky and Osterkamp (1997).

Model evaluation at local sites

The deterministic modeling approach described above was tested at an array of individual 1 ha Circumpolar Active Layer Monitoring (CALM) study areas (Figure 1), using site-specific parameters. Each of these sites was selected to represent homogeneous landcover categories characteristic of those in the two dominant physiographic provinces of the North Slope of Alaska: the Arctic Coastal plain and the Arctic Foothills (Wahrhaftig 1965). The dominant landcover classes in the study area are moist acidic tundra (MAT) and moist non-acidic tundra (MNT), together accounting for almost half of the surface cover in the North Slope's two physiographic provinces. MNT and wet tundra (WET) are extensive in the Coastal Plain province, while MAT and shrublands (SHR) are the predominant cover types in the Foothills (Walker and Muller 1999). Detailed site characterizations can be found in Walker and Bockheim (1995), Nelson *et al.* (1997), Bockheim *et al.* (1998), Shiklomanov and Nelson (1999), and Klene *et al.* (2001). Table 2 provides summary site descriptions.

The model used site-specific climate, thickness of vegetation, organic layer, and the snow and thermal properties parameterizations outlined above. Table 3 summarizes results from the site-specific modeling. Although this equilibrium modeling approach implies steady-state conditions and cannot be used on an annual basis, the model provides reasonable estimates of long-term average values of ALT.

Because CALM sites are representative of a variety of climatic and landscape conditions, it is possible to extrapolate the modeling results from site-specific scales to landscape or landcover-specific scales (Nelson *et al.* 1997; Shiklomanov and Nelson 2002). This allows construction of landcover-specific distributions of ALT by grouping sites according to their positions in particular landscapes. Extensive analysis of observational data (e.g. Streletskiy *et al.* 2008) has shown that similar landscapes have similar values of ALT, while different landscapes have distinctly different ALT distributions. The particular distribution in each landscape is attributed to a particular combination of edaphic parameters, meaning that climatic conditions influence the central tendency of ALT values, but not the overall landscape-specific distribution. Hence, by minimizing climatic variability (using climatic averages), the landscape-specific distribution of ALT will be attributed primarily to the landscape-specific factors. At the regional scale, variability of climatic conditions can be minimized by comparing different landscapes in similar climatic conditions. In the case of the North Slope of Alaska, monthly temperature means, available from the observational network and averaged for the 1995–2008 period, were used to minimize the temporal climatic influence.

The deterministic model used for site-specific modeling was based on a single parameter–single value scheme, as average input parameters were assumed for every location. For smaller scale applications, a stochastic algorithm should be built into

Table 2. Site-specific input characteristics used in active-layer modeling.

ID	Landcover class	Coordinates	Elev. (m)	Soil texture	Moss (cm)	Peat (cm)	W (%)
U7B	MNA	N70 17, W148 54	12	Loam	1.8	12	54
U7C	WET	N70 16, W148 55	12	Loam	0.8	25	74
U32A	MNA	N69 26, W148 40	269	Silty loam	2.1	9	35
U32B	MAT	N69 24, W148 40	360	Silty clay	2.2	15	51
U12B	MAT/WET	N68 37, W149 37	777	Loam	1.8	15	51
U11B	WET	N68 37, W149 19	917	Loam	2	34	46
U11C	MAT	N68 37, W149 19	938	Silty clay	2.5	15	51
U10	SHR/WT	N69 08, Wl48 36	537	Loam	3.2	19	51

Note: Detail description can be found under corresponding sites at www.udel.edu/Geography/calm.

Table 3. Predicted and observed values of ALT for CALM 1-ha plots in Northern Alaska for the 1995–2007 period.

ID	Landcover class	Tair	dTv	dTs	dTof	TTOP	Predicted ALT (cm)	Observed ALT (cm)
U7B	MNA	−11.2	−0.2	3.2	0.0	−8.2	40	39
U7C	WET	−10.9	−0.1	4.1	0.0	−6.9	31	41
U32A	MNA	−9.2	−0.4	3.0	−0.1	−6.6	59	56
U32B	MAT	−9.4	−0.4	4.1	−0.3	−5.9	40	37
U12B	MAT/WET	−7.9	−0.3	4.0	−0.3	−4.5	46	43
U11B	WET	−7.8	−0.3	3.8	−0.1	−4.5	50	49
U11C	MAT	−7.0	−0.4	3.7	−0.3	−3.9	43	42
U10	SHR/WT	−8.5	−0.6	4.0	−0.1	−5.1	45	43

Note: Tair – mean annual temperature, dTv – annual effect of vegetation on ground surface temperature, dTs – annual effect of snow cover on ground surface temperature, dTof – thermal offset, TTOP –temperature of permafrost table.

the model, as input edaphic parameters can be quite variable even between similar landscapes. The number of landscape variables (k) was set to six: snow cover height, moss height, organic layer thickness, soil moisture content, peat moisture content, and amount of peat in the ground. Soil bulk density and organic layer density were assumed to be constant within each landcover category. The initial parameters of the model were obtained from the available soil and vegetation surveys. This eliminated the possibility of applying unrealistic combinations of parameters to the model. Each input parameter was expressed as its minimum and maximum value, so that the number of ALT values (n) in each landcover class was equal to $n = 2^k = 64$. At the first step, the minimum and maximum ALT values were determined from the n-modeled samples. If the range of modeled values of ALT was similar to the observed range characteristic of a particular landcover category, the parameters responsible for the minimum and maximum values of ALT were averaged to produce a mean value of ALT. Input parameters were then set to vary around the mean value, to produce a statistical frequency distribution similar to the observed ALT distribution. The resulting characteristics of observed and modeled ALT are shown in figure 2. Results at the landscape scale indicate that the model is able to produce landcover-characteristic distributions of ALT when forced with vegetation and soil observational data. Snow and vegetation covers attenuate air temperature amplitude and create boundary conditions at the ground surface, which further defines the possible range of characteristic ALT within each particular landscape category. Soil and peat properties are responsible for deviations of ALT inside this range, creating a landscape-specific distribution of ALT.

Model application at regional scales

To evaluate the regional spatial variability of ALT over the North Slope of Alaska, the baseline period 1970–2000 was chosen as representative of contemporary climatic conditions. Snow depth was calculated from snow water equivalent (SWE) data derived from Scanning Multichannel Microwave Radiometer and selected Special Sensor Microwave/Imagers for the period 1978–2007 (Armstrong *et al.* 2007). SWE data from satellites were validated against an empirical relationship

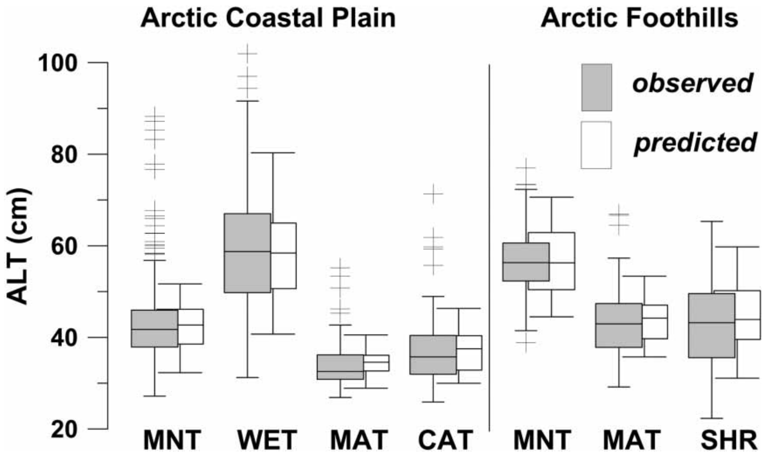

Figure 2. Predicted and observed landscape-specific ALT (cm) for the characteristic soil and vegetation associations of the two North Slope physiographic provinces. MNT – moist non-acidic tundra, MAT – moist acidic tundra, SHR – low shrub tundra and shrublands, WET – wet Graminoid tundra, CAT – cold acidic tundra.

developed by M. Sturm specifically for the Kuparuk region of Northern Alaska based on 56,000 point measurements of snow depth taken during March and April 1996 (Shiklomanov and Nelson 1999). The agreement was within 5 cm using snow density of 300 kg/m^3 (Streletskiy 2010).

The North Slope of Alaska was outlined as the terrestrial surface within the limits of 67–71°N and 140–167°W, resulting in an area of 0.368 million km^2. A map of Alaska (Walker and Muller 1999) with 100 m resolution (figure 3) was used as the basis for landcover classification. Each landcover class was parameterized according to specific vegetation and soil properties. Water accounts for almost 18% of the Coastal Plain province's area and less than 2% of the Foothills. Barrens occupy more than 10% of the Foothills but only 3% of the Coastal Plain (Walker and Muller 1999).

Active-layer thickness was initially calculated for the entire North Slope using the assumption that the area can be represented by a single landcover class. Water, shadows, and ice were excluded, resulting in a total of six model runs for the Barrens, MNT, MAT, SHR, WET, and CAT landcover classes. To estimate dataset-specific biases in ALT, this exercise was repeated four times, using four climatic datasets (CRU, ERA40, W&M, and NCEP). ALT was then calculated in accordance with the frequency distribution of 100 m landcover categories in each 625 km^2 climatic grid cell (figure 4). The resulting values were used to produce maps of contemporary geographic patterns and probabilities that the active layer exceeds certain thresholds for the North Slope of Alaska.

Projected active-layer thickness

To address potential changes in the active layer for the entire area of Alaska, the model was forced by the high-resolution climate dataset from Scenarios Network for Alaska Planning (SNAP 2012). The dataset is based on downscaled output from five IPCC GCMs in the region, and includes ensemble means of air

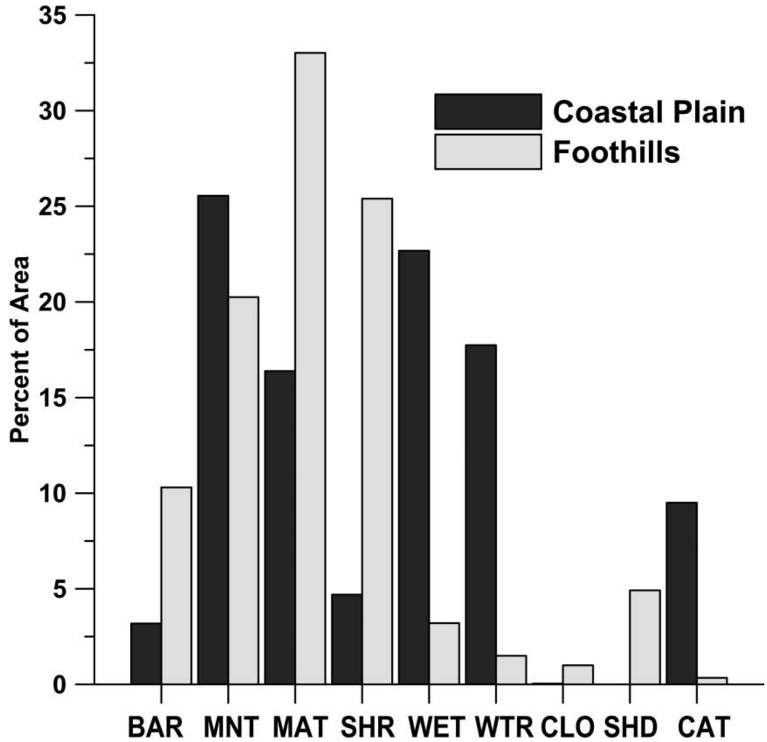

Figure 3. Percent cover by landcover classes for the entire North Slope of Alaska (NSA), Coastal Plain (CP) and Foothills (FH) provinces. BAR –barrens, MNT – moist non-acidic tundra, MAT – moist acidic tundra, SHR – low shrub tundra and shrublands, WET – wet Graminoid tundra, CAT – cold acidic tundra, WTR – water, CLO – clouds and ice, SHD – shadows. WTR, CLO and SHD classes are considered as no data pixels and are excluded from analysis.

temperature and precipitation from the ECHAM5, GFDL21, MIROC, HAD and CCCMA models for the A1B emission scenario. This scenario falls in the midrange of projections considered by IPCC and has the highest rates of technological change, economic development, and balanced energy use across all energy sources (IPCC 2000). The dataset spans the 1980–2099 period and covers the entire state of Alaska with a horizontal resolution of 2 km^2. The downscaling was performed using 'Parameter-elevation Regressions on Independent Slopes Mode' algorithm (PRISM 2012). The last decade of the twentieth century was chosen as a baseline for comparison and the last decade of the twenty-first century was used to provide the forecast.

The projected increase in both the duration of the growing season and of summer temperatures is likely to result in further greening of the Arctic, shrub expansion, and advance of forest vegetation species into the tundra zone of Alaska (Hinzman *et al.* 2005). This makes application of current landcover parameterizations unsuitable for modeling at the century time scale because changes in landscapes will occur, and because landscape properties are also likely to change. This introduces larger uncertainties in the model, already high because of the uncertainties in the climatic fields. To eliminate uncertainties associated with

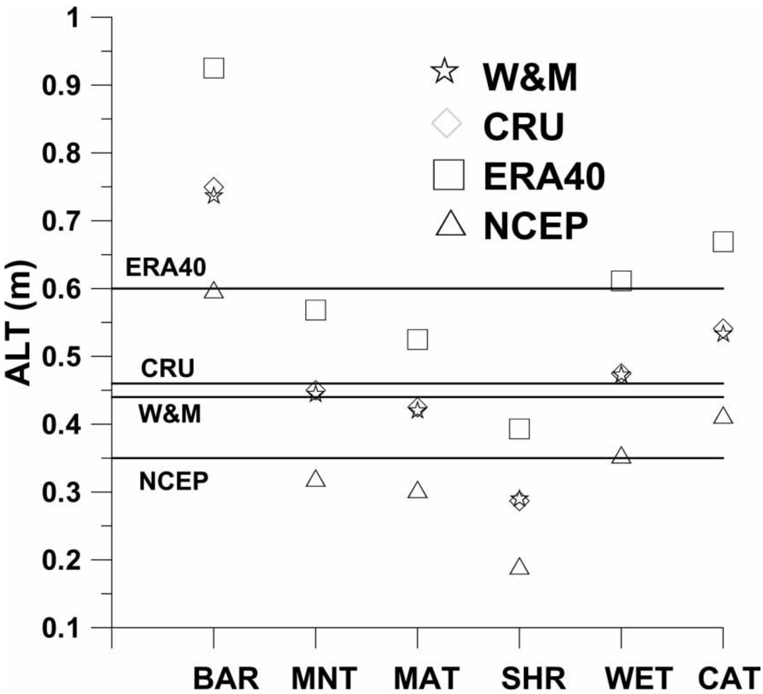

Figure 4. Regional estimates of ALT according to four climatic datasets assuming that the entire region is represented by a single landcover class (symbols) and weighted averages of regional ALT, based on the distribution of landcover classes within each climatic grid (solid lines).

potential landscape changes, a hypothetical soil profile was introduced. The profile contains a moss layer of 10 cm over a peat layer, atop a 10 cm sandy loam soil with low ice content. To eliminate uncertainties associated with vegetation redistribution, vegetation height of 10 cm was assumed for the entire region.

Results and discussion

Spatial variability of ALT under contemporary climate

Results indicate ALT increasing from north to south. This general trend is modified in the northern part of the Foothills province, however, where MAT and shrublands provide more thermal insulation compared with MNT, resulting in shallower active layers despite warmer temperatures (figure 5). This agrees well with the observational results of Walker *et al.* (2003).

The western part of the North Slope has a smaller range of ALT than does the eastern part. This result is partially attributable to the fact that climate datasets have better agreement in the western part, although differences are found throughout the entire region. Comparison of the four climatic datasets revealed that, on average, ERA40 produces the warmest annual air temperature and NCEP produces the coldest, while observational datasets from CRU and W&M are closest to the mean of the four. As is evident from temperature comparisons, ERA40 produced the thickest regional ALT (0.6 m), while NCEP (0.35 m) produced the

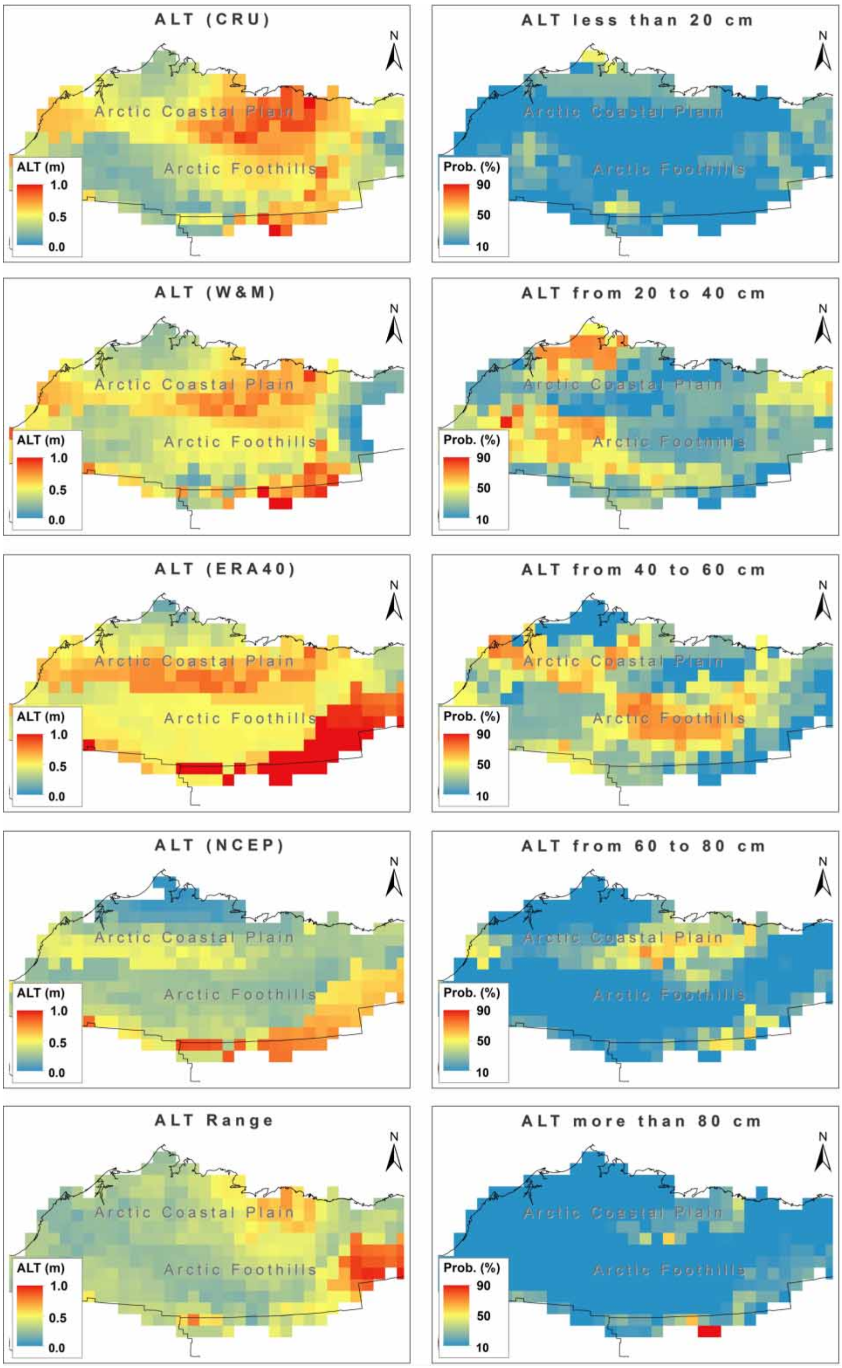

Figure 5. Geographic patterns of contemporary ALT and the range of values in the North Slope (left) and probability of active layer exceeding specified thresholds (right), derived from four climatic datasets. W&M – University of Delaware; CRU – University of East Anglia; ERA40 – European Center for Medium-Range Weather Forecast 40-year Re-Analysis; NCEP – National Center for Environmental Prediction–National Center for Atmospheric Research.

thinnest, with the two observational datasets showing mid-range values of ALT compared with reanalysis (figure 4). This shows that, depending on climatic input, estimates of regional ALT can be highly divergent. Probability maps therefore offer an advantage, as uncertainty associated with the climate data is already incorporated in the stochastic procedure used to evaluate probabilities of ALT to be within specified bounds. The series of maps of ALT for the North Slope of Alaska depicts the probability of the active layer exceeding specified thresholds (figure 5). Two classes (20–40 and 40–60 cm) show the highest probability of occurrence within the region, with the exception of the southern Foothills, where the probability of ALT being more than 80 cm is high because of the sparse vegetation in the barrens category.

Spatial variability of ALT under projected climate

Analysis of projected changes in air temperature and snow cover depth indicates that both surface and ground temperature will increase substantially by the end of the twenty-first century. Results from the model forced with the A1B emission scenario indicate that temperature at the top of permafrost (TTOP) will increase substantially throughout Alaska by the end of the twenty-first century, especially north of the Brooks Range. Near-surface permafrost will disappear in the Alaskan interior, with the exception of high-elevation areas in the Alaska Range and a few other areas, such as the western Seward Peninsula. Tundra in the southern part of the North Slope will, according to this scenario, likely be underlain by discontinuous permafrost. In the northern part of the North Slope, the tundra will remain in the zone of continuous permafrost, but with substantially higher temperature than at present (in some cases up to 6.2°C higher).

Increases of near-surface permafrost temperature will be accompanied by changes in the active layer. Projected climate warming under the A1B scenario in Alaska will lead not only to increases in ALT in permafrost regions but also will create conditions under which the active layer will no longer reach the permafrost table. To address these changes it is useful to subdivide the active layer into a layer of 'seasonally thawed ground' overlying permafrost, and a layer of 'seasonally frozen ground' overlying unfrozen ground inside or outside permafrost areas (cf. van Everdingen 1998). Projected changes in the active layer can then be classified into three geographic zones (figure 6):

(1) A permafrost zone in which a seasonally thawed layer will become progressively thicker following increases in both summer temperatures and the duration of the thawing period by the end of the century (North Slope of Alaska, Brooks Range, high mountains of Alaska Range).
(2) A relict permafrost zone, the geographic position and extent of which correspond with the contemporary discontinuous and sporadic permafrost zones. In this zone, relict permafrost will remain below the surface, but the duration and intensity of the cold season will become progressively smaller, and by the end of the twenty-first century will not be sufficient to reach the permafrost table. This will create a vertically discontinuous permafrost profile consisting of a seasonally frozen layer, a residual thaw layer, and permafrost. Relict permafrost will be present between the Alaska Interior (north of 66°N) and the Brooks Range.

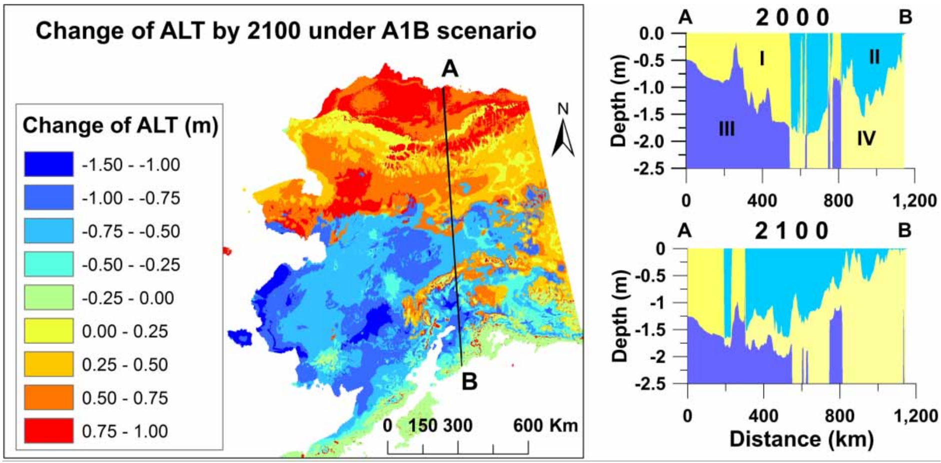

Figure 6. Geographic patterns of projected changes in ALT by the end of twenty-first century under A1B emission scenario and generalized permafrost profile along 150 W. I – seasonal thawing, II – seasonal freezing, III – permafrost, IV – no permafrost.

(3) A permafrost-free zone with a progressively decreasing seasonally frozen layer, reflecting both increased winter temperatures and decreased duration of freezing. This zone will occupy most of the Alaskan Interior south of 66°N.

Comparison of temperature profiles for the twenty-first century shows a general shift toward higher ground surface temperatures, interpreted as a contraction of the area with a layer of seasonally thawed ground over permafrost and an increase of the area with a layer of seasonally frozen ground and no underlying permafrost. Under the prescribed landscape conditions, ground surface temperature will rise by higher than 2–3°C by 2050, with most of the warming attributed to the minimum values (cold permafrost becoming warmer). This agrees with current observational trends, which show more rapid warming of cold permafrost (Romanovsky *et al.* 2010). By 2100, the changes in ground surface temperature will be substantial (4.5–6.2°C). The geographic extent of areas with TTOP lower than −4°C will be negligible. Predicted percentage changes of areas with seasonally frozen and thawed layers show a gradual increase in the area currently occupied by seasonally frozen ground and a decrease of areas currently occupied by seasonally thawed ground (Table 4). Areas with seasonal freezing show a significantly slower increase than does the decrease of areas with seasonal thawing. If the projected layer of seasonally frozen ground does not reach the contemporary permafrost table (approximated as the maximum possible seasonally thawed layer in 2000), development of a residual thaw layer will begin, resulting in a widespread three-layer vertical profile by the end of the twenty-first century (i.e. a zone of relict permafrost).

To demonstrate the changes in ALT by 2100, a north–south profile across Alaska at 150°W was constructed (A and B in figure 6). The upper right portion of figure 6 shows the profile for the last decade of the twentieth century, while the lower right shows the profile for the last decade of the twenty-first century. The twentieth-century profile shows two roughly equal zones – a zone of seasonal thawing in the northern half of the state and zone of seasonal freezing in the southern half. The zone of general seasonal freezing is intersected by a few locations with seasonal

Table 4. Percentage changes of area under seasonal freezing and seasonal thawing relative to 2000 under A1B scenario in Alaska.

	Area (%)	
Year	Freezing	Thawing
2000	100	100
2025	111	82
2050	130	50
2075	138	40
2100	144	28

thawing in alpine permafrost environments characteristic for high elevations. By the end of the twenty-first century, most of the North Slope will have a significantly thicker layer of seasonal thawing. The southern part will experience seasonal freezing, which will be unable to reach the permafrost table, and thaw development of the upper permafrost will occur. Most parts of the Brooks Range will remain a permafrost environment. The Alaskan interior will be dominated by seasonal freezing processes. The annual cold wave at the surface will be insufficient for freezing to reach the permafrost table, so a three-layer permafrost system is likely to develop: a layer of seasonal freezing, a thaw layer, and permafrost. According to the model, the thawed layer will not be more than 1–2 m thick, so a few cold winters have the potential to re-establish a vertically continuous permafrost profile.

Conclusions

This study used a stochastic approach, in combination with an equilibrium permafrost model, to map the spatial distribution of contemporary ALT on the North Slope of Alaska. For a given location, differences in ALT produced by the four climate datasets used in this study are equivalent to those observed over several degrees of latitude, or between starkly contrasting landscapes such as unvegetated barrens and areas with well-developed vegetation cover. Over the region as a whole, the climate datasets produce an average difference of 0.15 m.

A major advantage of the stochastic approach lies in its integration of all possible combinations of climatic and landscape variables to produce probabilistic maps of contemporary ALT. The largest uncertainties in this study are associated with landscape transformations, particularly those involving changes in surface cover, accompanying future climatic change. However, the approach employed here has potential for use with an ensemble of climatic projections to estimate the potential for the active-layer to exceed specified thresholds. Under the climate change projected by the A1B scenario, near-surface permafrost will disappear south of the Brooks Range, while on the North Slope the active layer will thicken substantially.

The integrated approach used in this study, based on observational data, modeling, and GIS techniques, can readily be applied in other Arctic regions containing permafrost. The modeling strategy has potential for use in areas where climatic and landscape conditions are known but observational active-layer data are unavailable.

Acknowledgements

We thank Cort Willmott (University of Delaware), Dmitry Drozdov (Russian Academy of Sciences), and Skip Walker (University of Alaska-Fairbanks) for reviewing an earlier version of this paper. This research was sponsored by the US National Science Foundation grant ARC-1002119 to the George Washington University, and NASA grants NNX09AI94G and 09-040 to the George Washington University, the University of Delaware and the University of New Hampshire. Opinions, findings, conclusions, and recommendations expressed in this paper are those of the authors, and do not necessarily reflect the views of NSF or NASA.

References

ACIA, 2004, *Impacts of a Warming Arctic: Arctic Climate Impact Assessment* (New York: Cambridge University Press).

Anisimov, O.A., and Reneva, S., 2006, Permafrost and changing climate: the Russian perspective. *Ambio*, **35**(4), pp. 169–175.

Anisimov, O.A., Shiklomanov, N.I., and Nelson, F.E., 1997, Global warming and active-layer thickness: results from transient general circulation models. *Global and Planetary Change*, **15**, pp. 61–77.

Anisimov, O.A., Shiklomanov, N.I., and Nelson, F.E., 2002, Variability of seasonal thaw depth in permafrost regions: a stochastic modeling approach. *Ecological Modelling*, **153**(3), pp. 217–227.

Armstrong, R.L., Brodzik, M.J., Knowles, K., and Savoie, M., 2007, *Global Monthly EASE-Grid Snow Water Equivalent Climatology* (Boulder, CO: National Snow and Ice Data Center).

Arzhanov, M.M., Eliseev, A.V., Demchenko, P.F., and Mokhov, I.I. 2007, Modeling of changes in temperature and hydrological regimes of subsurface permafrost using the climate data (reanalysis). *Earth Cryosphere*, **11**(4), pp. 65–69 (in Russian).

Beringer, J., Lynch, A.H., Chapin III, F.S., Mack, M., and Bonan, G., 2001, The representation of Arctic soils in the land surface model: the importance of mosses. *Journal of Climate*, **14**, pp. 3324–3335.

Bockheim, J.G., Walker, D.A., Everett, L.R., Nelson, F.E., and Shiklomanov, N. I., 1998, Soils and cryoturbation in moist nonacidic and acidic tundra in the Kuparuk River Basin, Arctic Alaska, U.S.A. *Arctic and Alpine Research*, **30**(2), pp. 166–174.

Brown, R.J.E., 1970, Occurrence of permafrost in Canadian peatlands. *Proceedings of the Third International Peat Congress, Quebec*, pp. 174–181 (Ottawa: National Research Council of Canada).

Brown, R.J.E., and Williams, G.P., 1972, The freezing of peatland. National Research Council of Canada, Technical Paper of the Division of Building Research, vol. **381**, 24 pp.

Callaghan, T.V., Tweedie, C.E., and Webber, P.J., 2011, Multi-decadal changes in tundra environments and ecosystems: the International Polar Year-Back to the Future Project (IPY-BTF). *Ambio*, **40**(6), pp. 555–557.

Chernad'ev, V.P., Chehovskiy, A.L., Stremyakov, A.Y., and Pakulin, V.A., 1984. Forecast of thermal state of ground under development of northern regions. Moscow, Nauka Press, 137 pp. (in Russian).

CNR, 1990, *Stoitelnie Normi i Pravila* [Construction Norms and Regulations]. Foundations on Permafrost 2.02.04-88. State Engineering Committee of the USSR, 56 pp (in Russian).

Duchkov, A.D., and Balobaev, V.T., 1998, Geothermal studies of permafrost response to global natural changes. In *Proceedings of the NATO Advanced Research Workshop on*

Permafrost Response on Economic Development, Environmental Security and Natural Resources, Novosibirsk, Russia, R. Paepe and V. Melnikov (Eds.) pp. 317–331, 12–16 November (Dordrechet: Kluwer Academic Publishers).

ERSHOV, E.D., 2002, *Fundamentals of Geocryology* (Moscow: Moscow State University Press), 682 pp (in Russian).

FAROUKI, O.T., 1981, *Thermal Properties of Soils* (Hanover: US Army Cold Regions Research and Engineering Laboratory). Monograph 81–1.

FELDMAN, G.M., 1977, *Forecast of Ground Temperature Regime and Development of Cryogenic Processes* (Nauka: Novosibirsk), 192 pp (in Russian).

FELDMAN, G.M., TETELBAUM, A.S., SHENDER, N.I., and GAVRILIEV, R.I., 1988, *Handbook on Ground Temperature Regime Forecast of Yakutia* (Yakutsk: SB RAS). 204 pp (in Russian).

GAVRILIEV, R.I., 2003, Quantitative estimation of the thermal conductivity of saturated frozen soils. In *Proceedings of the Eighth International Conference on Permafrost, Zurich, Switzerland*, vol. 1, pp. 283–285, 21–25 July (Rotterdam, NL: A.A. Balkema Publishers).

GOODRICH, L.E., 1982, The influence of snow cover on the ground thermal regime. *Canadian Geotechnical Journal*, **19**, pp. 421–432.

GUTMAN, G., and REISSELL, A. (Eds.), 2010, *Eurasian Arctic Land Cover and Land Use in a Changing Climate* (New York: Springer), 226 pp.

HINZMAN, L.D., KANE, D.L., GIECK, R.E., and EVERETT, K.R., 1991, Hydrologic and thermal properties of the active layer in the Alaskan arctic. *Cold Regions Science and Technology*, **19**(2), pp. 95–110.

HINZMAN, L.D., BETTEZ, N.D., BOLTON, W.R., CHAPIN, F.S., DYURGEROV, M.B., FASTIE, C.L., GRIFFITH, B., HOLLISTER, R.D., HOPE, A., HUNTINGTON, H.P., JENSEN, A.M., JIA, G.J., JORGENSON, T., KANE, D.L., KLEIN, D.R., KOFINAS, G., LYNCH, A.H., LLOYD, A.H., MCGUIRE, A.D., NELSON, F.E., OECHEL, W.C., OSTERKAMP, T.E., RACINE, C.H., ROMANOVSKY, V.E., STONE, R.S., STOW, D.A., STURM, M., TWEEDIE, C.E., VOURLITIS, G.L., WALKER, M.D., WALKER, D.A., WEBBER, P.J., WELKER, J.M., WINKER, K., and YOSHIKAWA, K., 2005, Evidence and implications of recent climate change in Northern Alaska and other Arctic Regions. *Climatic Change*, **72**, pp. 251–298.

IPCC, 2000, Intergovernmental Panel on Climate Change Special Report: Emissions Scenarios. Available at: http://www.ipcc.ch/pdf/special-reports/spm/sres-en.pdf (Accessed 3 January 2012).

KALNAY, E., KANAMITSU, M., KISTLER, R., COLLINS, W., DEAVEN, D., GANDIN, L., IREDELL, M., SAHA, S., WHITE, G., WOOLLEN, J., ZHU, Y., LEETMAA, A., REYNOLDS, R., CHELLIAH, M., EBISUZAKI, W., HIGGINS, W., JANOWIAK, J., MO, K.C., ROPELEWSKI, C., WANG, J., JENNE, R., and JOSEPH, D., 1996, The NCEP/NCAR 40-year reanalysis project. *Bulletin of American Meteorological Society*, **77**, pp. 437–471.

KLENE, A.E., NELSON, F.E., and SHIKLOMANOV, N.I., 2001, The n-factor as a tool in geocryological mapping: seasonal thaw in the Kuparuk River basin, Alaska. *Physical Geography*, **22**(6), pp. 449–466.

KONOVALOV, A.A., and ROMAN, L.T., 1973, The thermophysical properties of peat soils. *Osnovaniya, Fundamenty i Mekhanika Gruntov*, **3**, pp. 21–22.

KUDRYAVTSEV, V.A., GARAGULA, L.S., KONDRAT'YEVA, K.A., and MELAMED, V.G., 1974, *Osnovy Merzlotnogo Prognoza* (Basics of Permafrost Forecasting). (Moscow: Moscow State University Press), 431 pp (in Russian).

KUJALA, K., SEPPÄLÄ, M., and HOLAPPA, T., 2008, Physical properties of peat and palsa formation. *Cold Regions Science and Technology*, **52**, pp. 408–414.

LAWRENCE, D.M., and SLATER, A., 2005, A projection of severe near-surface permafrost degradation during the 21st century. *Geophysical Research Letters*, **32**, p. L24401.

Lawrence, D.M., and Slater, A., 2008, Incorporating organic soil into a global climate model. *Climate Dynamics*, **30**, pp. 145–160.

Macdonald, G.M., Beilman, D.W., Kremenetski, K.V., Sheng, Y., Smith, L.C., and Velichko, A.A., 2006, Rapid development of the Circumarctic peatland complex and atmospheric CH4 and CO2 variations. *Science*, **314**, pp. 285–288.

Malevsky-Malevich, S.P., Molkentin, E.K., Nadyozhina, E.D., Pavlova, T.P., and Semioshina, A.A., 2006, Validation problems of permafrost evolution modeling. *In* Melnikov, V.P. (Ed.), *Proceedings of International Conference: Earth Cryosphere Assessment: Theory, Applications and Prognosis of Alterations*, vol. 1, Tumen: Oilgas University Press, pp. 78–82, 29-31 May.

Marchenko, S., Romanovsky, V., and Tipenko, G., 2008, Numerical modeling of spatial permafrost dynamics in Alaska. *In* Kane, D.L., and Hinkel, K.M. (Eds.), *Proceedings of the Ninth International Conference on Permafrost*, vol. 2. Fairbanks: University of Alaska Press, pp. 1125–1130, 29 June to 3 July.

Mitchell, T.C., and Jones, P.D., 2005, An improved method of constructing a database of monthly climate observations and associated high-resolution grids. *International Journal of Climatology*, **25**, pp. 693–712.

Nelson, F.E., 1986, Permafrost in central Canada: applications of a climate-based predictive model. *Annals of the Association of American Geographers*, **76**(4), pp. 550–569.

Nelson, F.E., Anisimov, O.A., and Shiklomanov, N.I., 2002, Climate change and hazard zonation in the circum-Arctic permafrost regions. *Natural Hazards*, **26**, pp. 203–225.

Nelson, F.E., Shiklomanov, N.I., Mueller, G.R., Hinkel, K.M., Walker, D.A., and Bockheim, J.B., 1997, Estimating active-layer thickness over a large region: Kuparuk river basin, Alaska, U.S.A. *Arctic and Alpine Research*, **29**(4), pp. 367–378.

Nelson, F.E., Outcalt, S.I., Goodwin, C.W., and Hinkel, K.M., 1985, Diurnal thermal regime in a peat-covered palsa, Toolik Lake, Alaska. *Arctic*, **38**(4), pp. 310–315.

Nelson, F.E., Shiklomanov, N.I., and Mueller, G.R., 1999, Variability of active-layer thickness at multiple spatial scales, north-central Alaska, U.S.A. *Arctic, Antarctic, and Alpine Research*, **31**(2), pp. 158–165.

Oberman, N.G., and Shesler, I.G. 2009, Observed and projected changes in permafrost conditions within the European North-East of the Russian Federation. *Problemy Severa i Arctiki Rossiiskoy Federacii* (Problems and Challenges of the North and the Arctic of the Russian Federation), **9**, pp. 96–106 (in Russian).

Pavlov, A.V., 1994, Current changes of climate and permafrost in the Arctic and sub-Arctic of Russia. *Permafrost and Periglacial Processes*, **5**, pp. 101–110.

PRISM, 2012, Parameter-elevation Regressions on Independent Slopes Model. Available at: http://prism.oregonstate.edu/(Accessed 3 January 2012).

Riseborough, D.W., and Burn, C.R., 1988, Influence of an organic mat on the active layer. *Proceedings of the Fifth International Conference on Permafrost, Trondheim, Norway*, pp. 633–38 (Trondheim: Tapir Publishers).

Romanovsky, V.E., and Osterkamp, T.E., 1997, Thawing of the active layer on the coastal plain of the Alaskan Arctic. *Permafrost and Periglacial Processes*, **8**(1), pp. 1–22.

Romanovsky, V.E., and Osterkamp, T.E., 2001, Permafrost changes and impacts. In *Proceedings of the NATO Advanced Research Workshop on Permafrost Response on Economic Development, Environmental Security and Natural Resources, Novosibirsk, Russia*, R. Paepe and V. Melnikov, pp. 297–316, 12–16 November (Dordrechet: Kluwer Academic Publishers).

Romanovsky, V.E., Smith, S.L., and Christiansen, H.H., 2010, Permafrost thermal state in the polar Northern Hemisphere during the International Polar Year 2007–2009: a synthesis. *Permafrost and Periglacial Processes*, **21**, pp. 106–116.

Sazonova, T.S., and Romanovsky, V.E., 2003, A model for regional-scale estimation of temporal and spatial variability of active layer thickness and mean annual ground temperatures. *Permafrost and Periglacial Processes*, **14**, pp. 125–139.

SCHUUR, E.A.G., BOCKHEIM, J., CANADELL, J.G., EUSKIRCHEN, E., FIELD, C.B., GORYACHKIN, S.V., HAGEMANN, S., KUHRY, P., LAFLEUR, P.M., LEE, H., MAZHITOVA, G., NELSON, F. E., RINKE, A., ROMANOVSKY, V.E., SHIKLOMANOV, N., TARNOCAI, C., VENEVSKY, S., VOGEL, J.G., and ZIMOV, S.A., 2008, Vulnerability of permafrost carbon to climate change: implications for the global carbon cycle. *BioScience*, **58**(8), pp. 701–714.

SHARRAT, B., 1997, Thermal conductivity and water retention of a black spruce forest floor. *Soil Science*, **162**, pp. 576–582.

SHENDER, N.I., 1986. Recommendations of temperature forecast of soils (examples from central and eastern parts of Baikal-Amur zone). Yakutsk, Permafrost Institute, 57 pp. (in Russian).

SHIKLOMANOV, N.I., and NELSON, F.E., 1999, Analytic representation of the active layer thickness field, Kuparuk River basin, Alaska. *Ecological Modelling*, **123**, pp. 105–125.

SHIKLOMANOV, N.I., and NELSON, F.E., 2002, Active-layer mapping at regional scales: a 13-year spatial time series for the Kuparuk Region, North-Central Alaska. *Permafrost and Periglacial Processes*, **13**, pp. 219–230.

SHIKLOMANOV, N.I., ANISIMOV, O.A., ZHANG, T., MARCHENKO, S.S., NELSON, F.E., and OELKE, C., 2007, Comparison of model-produced active layer fields: results for Northern Alaska. *Journal of Geophysical Research*, **112**, p. F02s10.

SNAP, 2012, Scenarios Network for Alaska and Arctic Planning. Available at: http://www.snap.uaf.edu (Accessed 3 January 2012).

STENDEL, M., ROMANOVSKY, V.E., CHRISTENSEN, J.H., and SAZONOVA, T., 2006, Using dynamical downscaling to close the gap between global change scenarios and local permafrost dynamics. In *Proceedings of International Conference: Earth Cryosphere Assessment: Theory, Applications and Prognosis of Alterations, Tumen'* vol. 1, pp. 104–107.

STRELETSKIY, D.A. 2010, Spatial and temporal variability of active-layer thickness at regional and circumpolar scales. Ph.D. Thesis. University of Delaware.

STRELETSKIY, D.A., SHIKLOMANOV, N.I., and NELSON, F.E., 2012, Permafrost, infrastructure and climate change: a GIS-based landscape approach. *Arctic, Antarctic and Alpine Research* (in press).

STRELETSKIY, D.A., SHIKLOMANOV, N.I., NELSON, F.E., and KLENE, A.E., 2008, Long-term active and ground surface temperature trends: 13 years of observations at Alaskan CALM sites. *In* KANE, D.L., and HINKEL, K.M. (Eds.), *Proceedings of the Ninth International Conference on Permafrost*, vol. 2. Fairbanks: University of Alaska Press, pp. 1727–1732, 29 June to 3 July.

STURM, M., HOLMGREN, J., KOENIG, M., and MORRIS, K., 1997, The thermal conductivity of seasonal snow. *Journal of Glaciology*, **43**(143), pp. 26–41.

UPPALA, S.M., KÅLLBERG, P.W., SIMMONS, A.J., ANDRAE, U., DA COSTA BECHTOLD, V., FIORINO, M., GIBSON, J.K., HASELER, J., HERNANDEZ, A., KELLY, G.A., LI, X., ONOGI, K., SAARINEN, S., SOKKA, N., ALLAN, R.P., ANDERSSON, E., ARPE, K., BALMASEDA, M.A., BELJAARS, A.C.M., VAN DE BERG, L., BIDLOT, J., BORMANN, N., CAIRES, S., DETHOF, A., DRAGOSAVAC, M., FISHER, M., FUENTES, M., HAGEMANN, S., HÓLM, E., HOSKINS, B.J., ISAKSEN, L., JANSSEN, P.A.E.M., MCNALLY, A.P., MAHFOUF, J-F., JENNE, R., MORCRETTE, J-J., RAYNER, N.A., SAUNDERS, R.W., SIMON, P., STERL, A., TRENBERTH, K.E., UNTCH, A., VASILJEVIC, D., VITERBO, P., and WOOLLEN, J., 2005, The ERA40 reanalysis. *Journal of the Royal Meteorological Society*, **131**, pp. 2961–3012.

VAN EVERDINGEN, R., (Ed.), 1998, revised May 2005. *Multi-language Glossary of Permafrost and Related Ground-ice Terms*. Boulder, CO: National Snow and Ice Data Center/World Data Center for Glaciology. Available at: http://nsidc.org/fgdc/glossary/ (Accessed 3 January 2012).

WAHRHAFTIG, C., 1965, *Physiographic Divisions of Alaska*, USGS Prof. Pap. 482, US. Govt. Print. Off., Washington, DC. 52 pp.

Walker, D.A., and Bockheim, J.G., 1995, *Vegetation-Soil Characterization at the 12 Flux Tower Sites*. ARCSS/LAII/Flux Study (Fairbanks, AK: LAII Science Management Office, University of Alaska, Fairbanks).

Walker, D.A., and Muller, S.V., 1999, *Land-cover Map of the North Slope of Alaska* (Boulder, CO: National Snow and Ice Data Center). Digital media.

Walker, D.A., Jia, G.J., Epstein, H.E., Raynolds, M.K., Chapin, F.S., Copass, C., Hinzman, L.D., Knudson, J.A., Maier, H.A., Michaelson, G.J., Nelson, F., Ping, C.L., Romanovsky, V.E., and Shiklomanov, N., 2003, Vegetation-soil-thaw-depth relationships along a low-Arctic bioclimate gradient, Alaska: Synthesis of information from the ATLAS studies. *Permafrost and Periglacial Processes*, **14**(2), pp. 103–123.

Williams, P.J., and Smith, M.W., 1989. *The Frozen Earth. Fundamentals of Geocryology*. Cambridge Press, 306 pp.

Willmott, C.J., and Matsuura, K., 1995, Smart interpolation of annually averaged air temperature in the United States. *Journal of Applied Meteorology*, **34**, pp. 2577–2586.

Willmott, C.J., and Matsuura, K., 2001, *Terrestrial Air Temperature and Precipitation: Monthly and Annual Time Series (1950–1999)*, Version 1.02. Available at: http://climate.geog.udel.edu/~climate/html_pages/archive.html (Accessed 3 January 2012).

Wisser, D., Marchenko, S., Talbot, J., Treat, C., and Frolking, S., 2011, Soil temperature response to 21st century global warming: the role of and some implications for peat carbon in thawing permafrost soils in North America. *Earth System Dynamics*, **2**, pp. 121–138.

Zhang, T., Osterkamp, T.E., and Stamnes, K., 1997, Effects of climate on the active layer and permafrost on the North Slope of Alaska, U.S.A. *Permafrost and Periglacial Processes*, **8**, pp. 45–67.